RCCNet: An Efficient Convolutional Neural Network for Histological Routine Colon Cancer Nuclei Classification

S H Shabbeer Basha, Soumen Ghosh, Kancharagunta Kishan Babu, Shiv Ram Dubey, Viswanath Pulabaigari, and Snehasis Mukherjee

arXiv:1810.02797v3 [cs.CV] 8 Jun 2019

Abstract—Efficient and precise classification of histological cell nuclei is of utmost importance due to its potential applications in the field of medical image analysis. It would facilitate the medical practitioners to better understand and explore various factors for cancer treatment. The classification of histological cell nuclei is a challenging task due to the cellular heterogeneity. This paper proposes an efficient Convolutional Neural Network (CNN) based architecture for classification of histological routine colon cancer nuclei named as RCCNet. The main objective of this network is to keep the CNN model as simple as possible. The proposed RCCNet model consists of $1,512,868$ learnable parameters which are significantly less compared to the popular CNN models such as AlexNet, CIFAR-VGG, GoogLeNet, and WRN. The experiments are conducted over publicly available routine colon cancer histological dataset "CRCHistoPhenotypes". The results of the proposed RCCNet model are compared with five state-of-the-art CNN models in terms of the accuracy, weighted average F1 score and training time. The proposed method has achieved a classification accuracy of 80.61% and 0.7887 weighted average F1 score. The proposed RCCNet is more efficient and generalized in terms of the training time and data over-fitting, respectively.

I. INTRODUCTION

The medical image analysis is one of the fundamental, applied, and active research area during the last few decades. The classification of medical images such as colon cancer is one of the most popular core research areas of the medical image analysis [1]. Categorization of tumors at the cellular level can help medical professionals to better understand the tumor characteristics which can facilitate them to explore various options for cancer treatment. Classifying cell nuclei from routine colon cancer (RCC) images is a challenging task due to cellular heterogeneity.

The American Cancer Society publishes colon cancer (also known as Colorectal cancer (CRC)) statistics every three years. The American Cancer Society Colorectal Cancer Facts & Figures 2017-2019 [2] reports the following. In 2017, in the USA, an estimation says that $95,520$ new cases of colon cancer were found out of which $50,260$ people died, which includes $27,150$ men and $23,110$ women. The colon cancer is the third most dangerous cancer which affects both men and

women. Thus, it is required to analyze the medical images for accurate colon cancer disease recognition.

Nucleus image classification has been applied to various histology related medical applications. Following are some recent attempts in applying image analysis or computer vision techniques in the medical domain. In 2014, Veta et al. [3] published a complete review article on breast cancer image analysis. Many researchers worked in the area of histological image analysis, a few of them are [4], [5]. Traditional machine learning methods have been employed by several researchers using handcrafted features obtained from histology images [6], [7]. Manually engineered features may not always represent the underlying structure of histology images. On the other hand, convolutional neural networks (CNNs) extract high-level and more semantic features automatically from the training data.

Recently, deep learning based approaches have achieved very promising performance in the field of computer vision and image analysis [8]. In 2012, Krizhevsky et al. [9] proposed a deep CNN model (called the AlexNet) consisting of 8 learnable layers for image classification. The AlexNet model is further extended to VGG-16 by Simonyan et al. [10] with 16 number of trainable layers. Later, the GoogLeNet with inception modules became popular for deep networks [11]. In recent development, He et al. [12] proposed a deeper residual network (ResNet) with 152 layers for image recognition in 2016. The CNN based models have also shown very encouraging performance for other tasks such as object detection, segmentation, depth estimation, and action recognition, etc. Girshick et al. [13] proposed R-CNN model (i.e., Regions with CNN features) for object detection. The 'You Only Look Once (YOLO)' model was proposed by Redmon et al. [14] for a unified, real-time object detection. Repala et al. [15] built a dual CNN based unsupervised model for depth estimation. Recently, Singh et al. [16] proposed Long Short-Term Memory (LSTM) networks and CNN based classifier to classify human actions.

The deep learning has been also utilized extensively for medical image and video analysis due to its capabilities to deal with complex data. In 2016, IEEE Transactions on Medical Imaging published a special issue on deep learning in medical imaging which focused on the achievement of CNN and other deep learning based approaches [17]. Litjens et al. [18] conducted a survey on deep learning in medical imaging by considering nearly 300 latest contributions, including image

Shabbeer Basha S.H., S. Ghosh, K.K. Babu, S.R. Dubey, Viswanath P., S. Mukherjee are with Computer Vision and Machine Learning Groups, Indian Institute of Information Technology, Sri City, Andhra Pradesh - 517646, India. email: {shabbeer.sh, soumen.g, kishanbabu.k, srdubey, viswanath.p, snehasis.mukherjee}@iiits.in
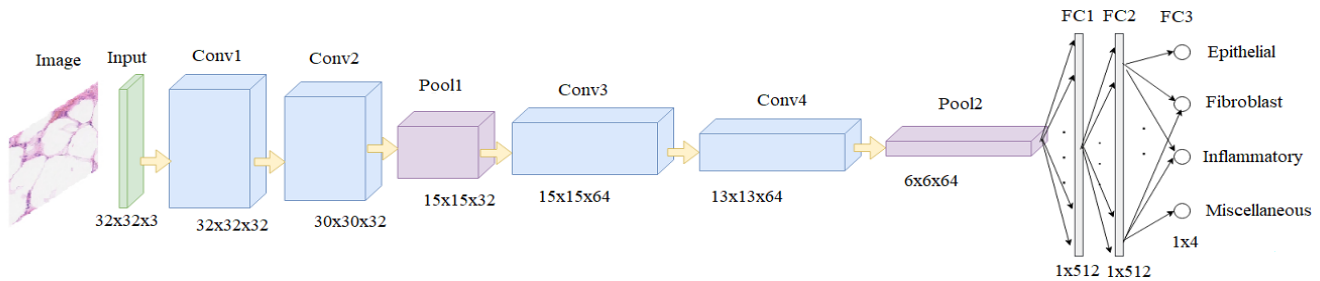
Fig. 1: Proposed RCCNet architecture for routine colon cancer nuclei classification. The first two convolutional layers (i.e., $Conv1$ and $Conv2$ layers) have 32 filters of size 3×3. The two convolutional layers in the middle (i.e., $Conv3$ and $Conv4$ layers) have 64 filters of size 3×3, each. The last three fully connected layers (i.e., $FC1$, $FC2$ and $FC3$ layers) have 512, 512, and 4 neurons, respectively. Two pooling layers (i.e., $Pool1$ and $Pool2$ layers) are used to down-sample the spatial dimension after $Conv2$ and $Conv4$ layers, respectively.

classification, object detection and segmentation tasks where deep learning techniques were used. Esteva et al. [19] proposed a deep CNN based classifier for skin cancer detection by training the model over a dataset of $1,29,450$ clinical images covering over $2,032$ different types of diseases. In 2017, Rajpurkar et al. [20] proposed CheXNet which is a 121 layer CNN model. The ChexNet model is trained over Chest X-ray14 dataset which is one of the largest publicly available chest X-ray dataset containing $1,00,000$ X-ray images belonging to 14 different diseases.

Xu et al. [21] proposed an unsupervised deep learning model called auto-encoder to classify cell nuclei, where the higher level features are classified using soft-max classifier. Korbar et al. [22] introduced a deep neural network model to classify different types of colorectal polyps in whole-slide images. Very recently, Bychkov et al. [23] proposed a classifier by combining the convolutional and recurrent neural network architectures for Colorectal cancer classification.

Sirinukunwattana et al. [1] proposed a convolutional neural network named as softmaxCNN_IN27 to classify cell nuclei in histology images. Their softmaxCNN_IN27 architecture has 5 trainable layers and $8,99,200$ learnable parameters. We have experimentally observed that the softmaxCNN_IN27 model used by Sirinukunwattana et al. [1] is not deep enough as compared to the complexity of the histology image dataset. To overcome this problem, we have proposed a deep CNN model named as RCCNet having 7 trainable layers with $1,512,868$ learnable parameters which outperforms softmaxCNN_IN27 [1] for the histological routine colon cancer nuclei classification task.

The main objective of this paper is to develop an efficient and simple CNN architecture suitable for the classification of histological colon cancer images. The simplicity considered is in terms of the number of layers and number of trainable parameters, which are compared against the widely used CNN models such as AlexNet, CIFAR-VGG, GoogLeNet and WRN. In this work, we figured out that a careful consideration of number of trainable layers and trainable parameters can lead to an efficient CNN model. The proposed model is called the RCCNet which is used for the RCC classification task. Experimentally, we compared the proposed method with other popular models such as softmaxCNN_IN27 [1], softmax-

CNN [1], AlexNet [9], CIFAR-VGG [24], GoogLeNet [11], and WRN [25]. A promising performance is observed using the RCCNet in terms of the efficiency and accuracy.

The rest of the paper is organized as follows. Section II is devoted to the detailed description of the proposed RCCNet architecture. Section III presents the experimental setup including dataset description along with a description of compared methods. Results and Analysis are reported in section IV. Finally, section V concludes the paper.

II. PROPOSED RCCNET ARCHITECTURE

Categorization of histology images is hard problem due to the high inter-class similarity and intra-class variablility. The primary objective of our work is to design a Convolutional Neural Network (CNN) based architecture which classifies the colon cancer images. This section describes the proposed RCCNet which has seven trainable layers.

The proposed RCCNet architecture is illustrated in Fig. 1. In the proposed architecture, we considered histology images of dimension $32 \times 32 \times 3$ as input to the network. This CNN model has three blocks with seven trainable layers. In the 1st block, two convolutional layers, viz., $Conv1$ and $Conv2$ are used just after the input layer. The $Conv2$ layer is followed by a pooling layer ($Pool1$) to reduce the spatial dimension by half. In the 2nd block, two convolutional layers (i.e., $Conv3$ and $Conv4$ layers) are followed by another pooling layer ($Pool2$). In the 3rd block, three fully connected layers, namely $FC1$, $FC2$, and $FC3$ are used in the proposed architecture. The input to 1st layer of 3rd block is basically the flattened features obtained from $Pool2$ layer. The 1st convolutional layer $Conv1$ produces a $32 \times 32 \times 32$ dimensional feature map by convolving 32 filters of dimension $3 \times 3 \times 3$. The zero padding by 1 pixel in each direction is done in $Conv1$ layer to retain the same spatial dimensional feature map. The $Conv2$ layer has the 32 filters of dimension $3 \times 3 \times 32$ with no padding which produces a $30 \times 30 \times 32$ dimensional feature map. The stride is set to 1 in both $Conv1$ and $Conv2$ layers. In $Pool1$ layer, the subsampling with the receptive field of 2×2 is applied with a stride of 2 and without padding which results in feature map of size $15 \times 15 \times 32$. The $Conv3$ layer produces 64 feature maps of spatial dimension 15×15 (i.e., spatial dimension is retained by applying zero padding with a factor of 1), which is obtained

by applying 64 filters of dimension $3 \times 3 \times 32$ with a stride of 1. Similar to $Conv2$ layer, $Conv4$ layer also does not apply padding and uses stride of 1. The $Conv4$ layer produces 64 features maps of dimension 13×13, obtained by convolving the 64 filters of size $3 \times 3 \times 64$. The second sub-sampling layer $Pool2$ also uses the kernel size of 2×2 with a stride of 2, which results in a $6 \times 6 \times 64$ dimensional feature map. The right and bottom border feature values of input are not considered in $Pool2$ layer to get rid of dimension mismatch between input and kernel size. The feature map generated by $Pool2$ layer is flattened into a single feature vector of length 2304 before 3rd block (i.e., fully connected layers). So, the input to $FC1$ layer is 2304 dimensional feature vector and output is 512 dimensional feature vector. Both input and output to $FC2$ layer is 512 dimensional feature vectors. The last fully connected layer $FC3$ takes the input of dimension 512 (i.e., the output of $FC2$ layer) and produces the 4 values as the output corresponding to the scores for 4 classes. This architecture consists of $1,512,868$ trainable parameters from 7 trainable layers (i.e., $Conv1$, $Conv2$, $Conv3$, $Conv4$, $FC1$, $FC2$, and $FC3$ layers).

On top of the last fully connected layer $FC3$ of proposed RCCNet model, a 'softmax classifier' for multi-class classification is used to generate the probabilities for each class. The probabilities generated by the 'softmax classifier' is further used to compute the loss during training phase and to find the predicted class during testing phase.

A. Training Phase

The categorical cross entropy loss is computed during the training phase. The parameters (weights) of the network are updated by finding the gradient of parameters with respect to the loss function. The cross-entropy loss (also known as the log loss) is used to compute the performance of a classifier whose output is a probability value ranging between 0 and 1. Let x be a three-dimensional input image to the network with class label $c \in C$ where $C = \{c_1, c_2, ...c_n\}$ is the set of class labels. In the current classification task, $C = \{1, 2, 3, 4\}$. The output of the network is a vector y which is,

$$y = f(x) \qquad (1)$$

where f denotes the forward pass computation function and $y = [y_1, y_2, ..., y_{c_n}]$ represents the class scores for the n classes. The cross-entropy loss for x, assuming that the target class (as given in the training set) is c_i,

$$L = -log\left(\frac{e^{y_i}}{\sum_{k=c_1}^{c_n} e^{y_k}}\right). \qquad (2)$$

The total loss over a mini-batch of training examples is considered in the training process.

B. Testing Phase

At test time, for a given input image, the class label having the highest score is the predicted class label. The predicted class label c_j is computed as,
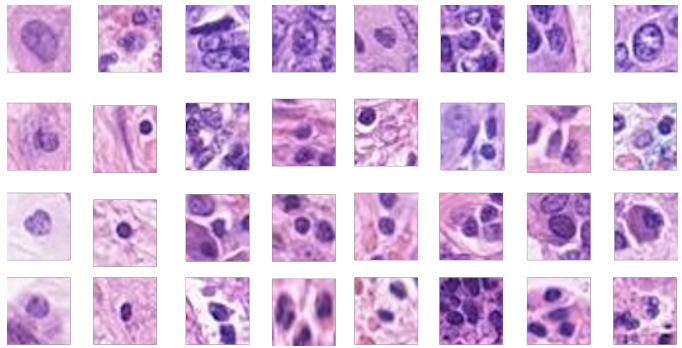
$$c_j = \arg \max_i p(y_i) \qquad (3)$$

Fig. 2: The sample patches from each class of "CRCHistoPhenotypes" dataset [1]. The 1st, 2nd, 3rd, and 4th rows show the patches from the classes, 'Epithelial', 'Fibroblast', 'Inflammatory', and 'Miscellaneous', respectively. The different columns in a row represent different samples from the same class.

where $p(y_i)$ is the probability that x belongs to class c_i, which is computed as follows.

$$p(y_i) = \frac{e^{y_i}}{\sum_{k=c_1}^{c_n} e^{y_k}}. \qquad (4)$$

III. EXPERIMENTAL SETUP

This section is devoted to present the experimental setting including dataset description, a briefing about the compared models, training details and the evaluation criteria.

A. Dataset Description

In order to find the performance of the proposed RCCNet for the task, we have used a publicly available 'CRCHistoPhenotypes' dataset[1] which consists of the histological routine colon cancer nuclei patches [1]. This dataset consists of 22444 nuclei patches that belong to the four classes, namely, 'Epithelial', 'Inflammatory', 'Fibroblast', and 'Miscellaneous'. In total, there are 7722 patches from the 'Epithelial' class, 5712 patches from the 'Fibroblast' class, 6971 patches from the 'Inflammatory' class and the remaining 2039 patches from the 'Miscellaneous' class. The dimension of each patch is $32 \times 32 \times 3$. The sample cell nuclei patches from the 'CRCHistoPhenotypes' dataset is given in Fig. 2.

B. Compared CNN Models

In order to justify the performance of the proposed RCCNet for the task, five state-of-the-art CNN models are implemented and a comparison is drawn. A brief overview of these architectures is given in the rest of this subsection.

1) softmaxCNN_IN27 [1]: Sirinukunwattana et al. [1] proposed softmaxCNN_IN27 architecture for the classification task. This model has 5 learnable layers including 2 convolutional and 3 fully connected layers. Each convolutional layer is followed by a max-pooling layer to reduce the spatial dimension by half. The 1st convolutional layer has 36 filters of size 4×4, which results in a feature map of dimension

---

[1]https://warwick.ac.uk/fac/sci/dcs/research/tia/data/crchistolabelednucleihe

$24 \times 24 \times 36$. The 1st max-pool reduces the dimension of feature map to $12 \times 12 \times 36$. The 2nd convolutional layer has 48 filters of kernel size 3×3, which produces a feature map of dimension $10 \times 10 \times 48$. The 2nd max-pooling produces the $5 \times 5 \times 48$ dimensional feature map. It is further followed by three fully connected layers, which have 512, 512, and 4 nodes, respectively. softmaxCNN_IN27 model consists of 899200 trainable parameters.

We also modified the architecture of sirinukunwattana et al. [1] with some minimal changes to make it suitable for $32 \times 32 \times 3$ dimensional input. It is called softmaxCNN. Initially, the input images are up-sampled to $33 \times 33 \times 3$. Then, zero padding by 1 pixel in each direction is done, which results in a $35 \times 35 \times 3$ dimensional image. The 1st convolution layer produces a $31 \times 31 \times 32$ dimensional feature map by convolving 32 filters of size $5 \times 5 \times 3$. This is followed by another convolution layer, which produces a $27 \times 27 \times 32$ dimensional feature map by applying 32 filters of size $5 \times 5 \times 32$. The rest of the architecture is same as the original softmaxCNN_IN27 [1]. softmaxCNN model consists of 944032 trainable parameters from 7 trainable layers.

2) AlexNet [9]: AlexNet [9] is the most popular CNN architecture, originally proposed for natural image classification. Initially we tried to make use of the original AlexNet [9] architecture by up-sampling the image dimension from $27 \times 27 \times 3$ to $227 \times 227 \times 3$. However, we experimentally observed no improvement even after training this model for 200 epochs. With this observation, we made minimal modifications to the AlexNet to fit for low resolution images. The image dimensions are up-sampled from $32 \times 32 \times 3$ to $33 \times 33 \times 3$. Then, zero padding by 1 pixel in each direction is done, which results in a $35 \times 35 \times 3$ dimensional image. This is followed by 1st convolution layer which produces a $31 \times 31 \times 96$ dimensional feature vector by applying 96 filters of dimension $5 \times 5 \times 3$. The 2nd convolutional layer produces the feature map of dimension $27 \times 27 \times 256$ by convolving 256 filters of dimension $5 \times 5 \times 96$. The rest of the architecture is same as original AlexNet [9] (the last fully connected layer is modified to have 4 neurons instead of 1000). This architecture corresponds to $197,731,396$ trainable parameters with 8 trainable layers.

3) CIFAR-VGG [10], [24]: Originally, the VGG-16 model was introduced by Simonyan et al. [10] for ImageNet challenge. Liu et al. [24] proposed a modified VGG-16 architecture (CIFAR-VGG) for training low scale images like CIFAR-10 [26]. We have utilized the CIFAR-VGG architecture [24] to train over histology images by changing the number of neurons in last FC layer to 4. This model has 16 trainable layers with $8,956,484$ trainable parameters.

4) GoogLeNet [11]: GoogLeNet [11] is the winner of ILSVRC 2014, which consists 22 learnable layers. GoogLeNet [11] is originally proposed for classification of large scale natural images. We made minimal changes to the GoogLeNet architecture [11] to work for low-resolution images. The 1st convolutional layer produces a $30 \times 30 \times 64$ dimensional feature map by applying 64 filters of dimension $3 \times 3 \times 3$. Then, 2nd convolution layer computes a $28 \times 28 \times 128$ dimensional feature map by applying 128 filters of dimension $3 \times 3 \times 64$. This is followed by an inception block, which results in a $28 \times 28 \times 256$ dimensional feature vector. The remaining part of the model is similar to original GoogLeNet [11] except the last fully connected layer which is is modified to have 4 neurons instead of 1000. This CNN model corresponds to $11,526,988$ trainable parameters.

5) WRN [25]: He et al. [12] introduced the concept of residual networks for natural image classification. Zagoruyko et al. [25] proposed a wide Residual Network (WRN) to train low resolution images of CIFAR-10 dataset. In this paper, we have adapted the WRN architecture [25] for comparison purpose. The number of nodes in the last fully connected layer is changed to 4 corresponding to the number of classes in used histology dataset. The WRN architecture used in this paper consists of $23,542,788$ trainable parameters.

C. Training Details

The initial value of the learning rate is considered as 6×10^{-5}, and iteratively decreased with a factor of $\sqrt[2]{0.1}$ if there is no improvement in validation loss during training. The rectified linear unit $(ReLU)$ [9] is employed as the activation function in all the implemented models. To reduce over fitting, dropout [27] is used after $ReLU$ of each fully connected layer with a rate of 0.5 and Batch Normalization [28] used after every trainable layer(except last FC layer) after $ReLU$ is applied. All the models are trained for 500 epochs using Adam optimizer [29] with $\beta_1 = 0.9$, $\beta_2 = 0.99$, and $decay = 1 \times 10^{-6}$. The 80% of entire dataset (*i.e.*, $17,955$ images) is used for the training and remaining 20% (*i.e.*, $4,489$ images) is used to test the performance.

D. Evaluation Criteria

In order to assess the performance of CNN models, we have considered two performance measures accuracy and weighted average F1 score. In this paper, the training time is also considered as one of the evaluation metrics to judge the efficiency of the CNN models.

IV. RESULTS AND ANALYSIS

We have conducted the extensive experiments to compare the performance of proposed RCCNet model with other state-of-the-art CNN models like softmaxCNN [1], AlexNet [9], CIFAR-VGG [24], GoogLeNet [11], and WRN [25]. Table I

TABLE I: The performance comparison of proposed RCCNet with state-of-the-art softmaxCNN_IN27, AlexNet[9], CIFAR-VGG[24], GoogLeNet[11], and WRN[25] models in terms of the Training Accuracy, Testing Accuracy, Overfitting %, Training F1 Score, and Testing F1 Score. The dimension of input images to softmaxCNN_IN27 model [1] is $27 \times 27 \times 3$, whereas for other models input size is $32 \times 32 \times 3$. The best accuracies and F1 scores are highlighted in **bold**.

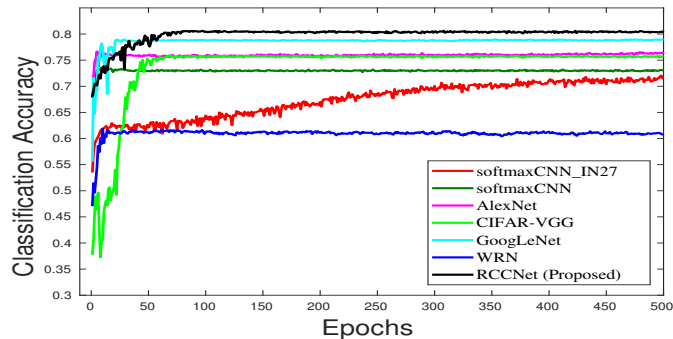| Model Name	#Trainable Parameters	Training Time (in minutes)	Classification Accuracy			Weighted Average F1 Score	
			Training Accuracy %	Testing Accuracy %	Overfitting %	Training F1 score	Testing F1 score
softmaxCNN_IN27 [1]	899,200	27.673	82.90	71.15	11.75	0.9332	0.7124
softmaxCNN [1]	944,032	28.774	83.63	73.71	9.92	0.9581	0.7439
AlexNet [9]	197,731,396	818.675	92.38	76.96	15.42	0.9897	0.7664
CIFAR-VGG [24]	8,956,484	102.259	85.43	75.94	9.49	0.9983	0.7708
GoogLeNet [11]	11,526,988	391.566	**99.99**	78.99	21.00	**0.9999**	0.7856
WRN [25]	23,542,788	77.829	98.61	61.88	36.73	0.9968	0.6227
RCCNet (Proposed)	1,512,868	31.404	89.79	**80.61**	**9.18**	0.9037	**0.7887**

Fig. 3: The Epoch wise test accuracies for different CNN models used in this paper for experiments.

presents the performance comparison among the CNN models in terms of the number of trainable parameters, training time, training accuracy, testing accuracy, amount of over-fitting, training F1 score, and testing F1 score. Followings are the main observations from the results of Table I:

1) The proposed RCCNet model outperforms the other CNN models both in terms of test accuracy and test weighted F1 score because the proposed model is highly optimized for histological routine colon cancer images.
2) The proposed RCCNet model has the lowest number of trainable parameters except softmaxCNN_IN27 and softmaxCNN [1]. Whereas, the AlexNet [9] model has largest number of learnable parameters.
3) The softmaxCNN model [1] proposed originally for histological routine colon cancer images is not enough complex, whereas our model is enough complex to produce a reasonable performance.
4) The proposed RCCNet model is better generalized as compared to other CNN models and results in lowest amount of over-fitting as depicted in Table I. The highest amount of over-fitting is observed for wide residual network (WRN) [25]. This analysis points out

that the amount of over-fitting is closely related to the network structure like depth of network, number of learnable parameters, and type of network (i.e., plain/inception/residual).
5) The test accuracy using RCCNet architecture is improved by 13.3%, 9.36%, 4.74 %, 2.05%, and 30.4% as compared to softmaxCNN_IN27 [1], softmaxCNN [1], AlexNet [9], GoogLeNet [11], and WRN [25] models, respectively due to the even size filters in softmaxCNN_IN27 and softmaxCNN [1] and high over-fitting occurred in other models.
6) The proposed RCCNet is more efficient in terms of the training time which is improved by 96.16%, 69.28%, 91.97%, and 56.64% as compared to AlexNet [9], CIFAR-VGG [24], GoogLeNet [11], and WRN [25], respectively due to the less number of learnable parameters and plain network architecture.

Fig. 3 shows the comparison among test accuracies of implemented CNN architectures. From Fig. 3, it is observed that the AlexNet [9], GoogLeNet [11] and WRN [25] converge quickly compared to other CNN architectures. The softmaxCNN_IN27 [1] model is slow in terms of the convergence. However, the proposed RCCNet architecture is very reasonable and converges smoothly.

V. CONCLUSION

In this paper, we have proposed an efficient convolutional neural network based classification model to classify colon cancer images. The proposed RCCNet model is highly compact and optimized for histological low-resolution patches. Only 7 plain trainable layers are used with $1,512,868$ trainable parameters. The classification experiments are performed over histological routine colon cancer patches. The performance of the proposed RCCNet model is compared with the other popular models like AlexNet, CIFAR-VGG, GoogLeNet, and WRN. The experimental results point out that the RCCNet is better generalizes and outperforms other models in terms of

5

the test accuracy and weighted average F1 score. The proposed RCCNet model attains 80.61% classification accuracy and 0.7887 weighted average F1 score. The RCCNet is also highly efficient in terms of the training time as compared to deeper and complex networks.

ACKNOWLEDGMENTS

REFERENCES

[1] K. Sirinukunwattana, S. E. A. Raza, Y.-W. Tsang, D. R. Snead, I. A. Cree, and N. M. Rajpoot, "Locality sensitive deep learning for detection and classification of nuclei in routine colon cancer histology images," *IEEE transactions on medical imaging*, vol. 35, no. 5, pp. 1196–1206, 2016.

[2] R. L. Siegel, K. D. Miller, S. A. Fedewa, D. J. Ahnen, R. G. Meester, A. Barzi, and A. Jemal, "Colorectal cancer statistics, 2017," *CA: a cancer journal for clinicians*, vol. 67, no. 3, pp. 177–193, 2017.

[3] M. Veta, J. P. Pluim, P. J. Van Diest, and M. A. Viergever, "Breast cancer histopathology image analysis: A review," *IEEE Transactions on Biomedical Engineering*, vol. 61, no. 5, pp. 1400–1411, 2014.

[4] M. Arif and N. Rajpoot, "Classification of potential nuclei in prostate histology images using shape manifold learning," in *Machine Vision, 2007. ICMV 2007. International Conference on*. IEEE, 2007, pp. 113–118.

[5] H. Sharma, N. Zerbe, D. Heim, S. Wienert, H.-M. Behrens, O. Hellwich, and P. Hufnagl, "A multi-resolution approach for combining visual information using nuclei segmentation and classification in histopathological images." in *VISAPP (3)*, 2015, pp. 37–46.

[6] T. R. Jones, A. E. Carpenter, M. R. Lamprecht, J. Moffat, S. J. Silver, J. K. Grenier, A. B. Castoreno, U. S. Eggert, D. E. Root, P. Golland *et al.*, "Scoring diverse cellular morphologies in image-based screens with iterative feedback and machine learning," *Proceedings of the National Academy of Sciences*, vol. 106, no. 6, pp. 1826–1831, 2009.

[7] H. Chang, A. Borowsky, P. Spellman, and B. Parvin, "Classification of tumor histology via morphometric context," in *Proceedings of the IEEE Conference on Computer Vision and Pattern Recognition*, 2013, pp. 2203–2210.

[8] Y. LeCun, Y. Bengio, and G. Hinton, "Deep learning," *nature*, vol. 521, no. 7553, p. 436, 2015.

[9] A. Krizhevsky, I. Sutskever, and G. E. Hinton, "Imagenet classification with deep convolutional neural networks," in *Advances in neural information processing systems*, 2012, pp. 1097–1105.

[10] K. Simonyan and A. Zisserman, "Very deep convolutional networks for large-scale image recognition," *arXiv preprint arXiv:1409.1556*, 2014.

[11] C. Szegedy, W. Liu, Y. Jia, P. Sermanet, S. Reed, D. Anguelov, D. Erhan, V. Vanhoucke, and A. Rabinovich, "Going deeper with convolutions," in *Proceedings of the IEEE conference on computer vision and pattern recognition*, 2015, pp. 1–9.

[12] K. He, X. Zhang, S. Ren, and J. Sun, "Deep residual learning for image recognition," in *Proceedings of the IEEE conference on computer vision and pattern recognition*, 2016, pp. 770–778.

[13] R. Girshick, J. Donahue, T. Darrell, and J. Malik, "Rich feature hierarchies for accurate object detection and semantic segmentation," in *Proceedings of the IEEE conference on computer vision and pattern recognition*, 2014, pp. 580–587.

[14] J. Redmon, S. Divvala, R. Girshick, and A. Farhadi, "You only look once: Unified, real-time object detection," in *Proceedings of the IEEE conference on computer vision and pattern recognition*, 2016, pp. 779–788.

[15] V. K. Repala and S. R. Dubey, "Dual cnn models for unsupervised monocular depth estimation," *arXiv preprint arXiv:1804.06324*, 2018.

[16] K. K. Singh and S. Mukherjee, "Recognizing human activities in videos using improved dense trajectories over lstm," in *Computer Vision, Pattern Recognition, Image Processing, and Graphics: 6th National Conference, NCVPRIPG 2017, Mandi, India, December 16-19, 2017, Revised Selected Papers 6*. Springer, 2018, pp. 78–88.

[17] H. Greenspan, B. van Ginneken, and R. M. Summers, "Guest editorial deep learning in medical imaging: Overview and future promise of an exciting new technique," *IEEE Transactions on Medical Imaging*, vol. 35, no. 5, pp. 1153–1159, 2016.

[18] G. Litjens, T. Kooi, B. E. Bejnordi, A. A. A. Setio, F. Ciompi, M. Ghafoorian, J. A. van der Laak, B. van Ginneken, and C. I. Sánchez, "A survey on deep learning in medical image analysis," *Medical image analysis*, vol. 42, pp. 60–88, 2017.

[19] A. Esteva, B. Kuprel, R. A. Novoa, J. Ko, S. M. Swetter, H. M. Blau, and S. Thrun, "Dermatologist-level classification of skin cancer with deep neural networks," *Nature*, vol. 542, no. 7639, p. 115, 2017.

[20] P. Rajpurkar, J. Irvin, K. Zhu, B. Yang, H. Mehta, T. Duan, D. Ding, A. Bagul, C. Langlotz, K. Shpanskaya *et al.*, "Chexnet: Radiologist-level pneumonia detection on chest x-rays with deep learning," *arXiv preprint arXiv:1711.05225*, 2017.

[21] J. Xu, L. Xiang, Q. Liu, H. Gilmore, J. Wu, J. Tang, and A. Madabhushi, "Stacked sparse autoencoder (ssae) for nuclei detection on breast cancer histopathology images," *IEEE transactions on medical imaging*, vol. 35, no. 1, pp. 119–130, 2016.

[22] B. Korbar, A. M. Olofson, A. P. Miraflor, C. M. Nicka, M. A. Suriawinata, L. Torresani, A. A. Suriawinata, and S. Hassanpour, "Looking under the hood: Deep neural network visualization to interpret whole-slide image analysis outcomes for colorectal polyps," in *Computer Vision and Pattern Recognition Workshops (CVPRW), 2017 IEEE Conference on*. IEEE, 2017, pp. 821–827.

[23] D. Bychkov, N. Linder, R. Turkki, S. Nordling, P. E. Kovanen, C. Verrill, M. Walliander, M. Lundin, C. Haglund, and J. Lundin, "Deep learning based tissue analysis predicts outcome in colorectal cancer," *Scientific reports*, vol. 8, no. 1, p. 3395, 2018.

[24] S. Liu and W. Deng, "Very deep convolutional neural network based image classification using small training sample size," in *Pattern Recognition (ACPR), 2015 3rd IAPR Asian Conference on*. IEEE, 2015, pp. 730–734.

[25] S. Zagoruyko and N. Komodakis, "Wide residual networks," *arXiv preprint arXiv:1605.07146*, 2016.

[26] A. Krizhevsky and G. Hinton, "Learning multiple layers of features from tiny images," 2009.

[27] N. Srivastava, G. Hinton, A. Krizhevsky, I. Sutskever, and R. Salakhutdinov, "Dropout: A simple way to prevent neural networks from overfitting," *The Journal of Machine Learning Research*, vol. 15, no. 1, pp. 1929–1958, 2014.

[28] S. Ioffe and C. Szegedy, "Batch normalization: Accelerating deep network training by reducing internal covariate shift," *arXiv preprint arXiv:1502.03167*, 2015.

[29] D. P. Kingma and J. Ba, "Adam: A method for stochastic optimization," *arXiv preprint arXiv:1412.6980*, 2014.